Forty Shades of Black: A Benchmark of High Temperature Sprayable Black Coatings Applied on Haynes 230

Simon Caron[1, a)], Jorge Garrido[2], Eneko Setien[3], Ridha Harzallah[4], Luka Noč[5], Ivan Jerman[5], Marc Röger[1], Florian Sutter[1]

[1]*German Aerospace Center (DLR), Institute of Solar Research, Plataforma Solar de Almería (PSA), Carretera de Senes km.5 , 04200 Tabernas, Spain*
[2]*Department of Energy Technology, KTH Royal Institute of Technology, SE-100 44 Stockholm, Sweden*
[3]*CIEMAT-PSA, Plataforma Solar de Almería (PSA), 04200 Tabernas, Spain*
[4]*John Cockerill, Avenue Greiner 1, 4100 Liège, Belgium*
[5]*National Institute of Chemistry, Hajdrihova 19, 1000 Ljubljana, Slovenia*

[a)] Corresponding author: simon.caron@dlr.de

Abstract. The solar receiver coating opto-thermal efficiency has a significant impact on a central receiver system thermal final system efficiency. The development of durable high solar absorptance coatings with simple application process and minimal thermal treatment can directly improve the receiver efficiency, thus reducing the levelized cost of electricity. During the past years, innovative receiver coatings for solar thermal tower plants have been developed on various substrates and tested under isothermal load at different temperature levels. In this paper, eight commercial black coating formulations are sprayed on Haynes 230 metal coupons. Solar absorptance and thermal emittance are monitored before and after isothermal exposure. Mass deviations are also measured to pinpoint any oxidation or coating outgassing. Isothermal testing is performed at 700, 750 and 800 °C in a muffle furnace for 1000 hours. After 1000 hours isothermal exposure, Coterill 750 leads the benchmark in front of Pyromark 2500, while other black coatings degrade optically. Uncoated samples oxidize significantly and appear darker than some aged black coatings.

INTRODUCTION

High temperature absorber coatings play a key role in the thermal efficiency of Central Receiver Systems (CRS). Pyromark 2500 is the state-of-the art coating [1] for external tube receiver designs, whose application can be further optimized [2,3]. Alternative innovative coating formulations have been recently developed and are being investigated [4,5,6]. The selection of a suitable receiver coating is driven by its opto-thermal performance, Levelized Cost of Coating (LCOC) and durability [7,8,9].

The most important optical parameter is the solar absorptance α_{sol}. For High Solar Absorptance (HSA) coatings, a stable value above 96% is required. Robust absorber coatings must withstand temperature levels above 700 °C for Gen3 CRS using new molten salt mixtures as a heat transfer fluid (HTF), with significant cyclic thermomechanical loads in operation. The coating application procedure has a significant impact on the LCOC. Re-coating and solar curing can be performed on site, on top of the tower at periodic intervals. Sprayable black coatings with minimal thermal treatment are thus preferred.

This paper aims to screen some commercial sprayable black coating formulations. The selected metal substrate is Haynes 230 (H230), which is currently one of the favorite substrate for CRS using molten salts as a HTF. Despite its high cost, H230 is a nickel-chromium (Ni-Cr) superalloy designed for high temperature applications such as gas turbines. H230 benefits from its excellent thermo-mechanical properties as well as its resistance against oxidation and corrosion [10] at high temperatures. In this paper, isothermal tests are performed in a muffle furnace for 1000 hours at 700, 750 and 800 °C in order to assess the optical degradation for each coating after isothermal exposure.

SolarPACES 2019
AIP Conf. Proc. 2303, 150007-1–150007-10; https://doi.org/10.1063/5.0028773
Published by AIP Publishing. 978-0-7354-4037-1/$30.00

MATERIALS AND METHODS

Substrate and Coatings

Forty-eight flat H230 coupons were prepared for the screening test campaign. These samples are allocated in ten sample sets. For each set, one reference sample is kept while other samples are respectively exposed at 700, 750 and 800 °C. The benchmark screens ten High Temperature (HT) coatings and two uncoated sample sets, one of which is sand blasted, while the other one is polished. Uncoated samples allow monitoring oxidation.

All sample sets are listed in Table 1 with relevant specifications regarding sample preparation. For each sample set, four samples are prepared in the same batch. One of the samples is kept as a reference (Pristine), while the three other samples are respectively exposed to 700, 750 and 800 °C for 1000 hours. The dimensions of flat metal coupons are: 50x45 mm^2, 2 mm thickness. For each metal coupon, approx. 10 mm is left uncoated on one edge. This uncoated edge is used for sample identification. It allows a visual comparison after testing, i.e. the contrast between the aged coating and the oxidized bare substrate allows determining whether the aged coating is qualitatively darker than the oxidized substrate.

TABLE 1. Inventory of coating variants screened the isothermal benchmark.

ID	Coating	Surface preparation	Rated maximum temperature (°C)	Coating procedure	Curing procedure
01	H230	Polished	1150 °C	Uncoated	-
02	H230	Sand blasting	1150 °C	Uncoated	-
03	Pyromark 2500 [1,2,3]	Sand blasting	< 1100 °C (2000 °F)	Internal, Spray gun	2 h @ 250 °C 1 h @ 540 °C
04	Lab-IR HT [11]	Sand blasting	1000 °C	Internal, Spray can	Air drying
05	Macota 3G-HT [12]	Sand blasting	800 °C	Internal, Spray can	Air drying
06	Cerakote Glacier Black C-7600Q [3]	None	~ 1100 °C (2000 °F)	External	Air drying
07	Senotherm UHT600 [14]	None	Min. 600 °C	External	Air drying
08	Aremco HiE-Coat 840-M (Metals) [15]	Sand blasting	~ 1100 °C (2000 °F)	Internal, Spray gun	1 h @ 100 °C
09	Aremco HiE-Coat 840 C (Ceramics) [15]	Sand blasting	~ 1100 °C (2000 °F)	Internal, Spray gun	Air drying
10	Slovenia NIC, Black 444 [5]	Sand blasting	Min. 800 °C	External	6 h @ 600 °C
11	Coterill 750 [6]	Sand blasting	750 °C	External	None
12	Pyromark 2500 [1,2,3]	Sand blasting	< 1100 °C (2000 °F)	External	2 h @ 250 °C

Sample sets (01-05,08,09) were applied at DLR workshop located at PSA, following recommendations provided by coating suppliers. Metal samples were sand blasted homogeneously, although precise surface roughness is unknown. Polishing (02) was performed manually using car polishing tools. Portable 400 mL spray cans were used for (04,05), applying 3-4 layers. A 400 mL spray gun with a 1.8 mm nozzle was used for coatings (03,08,09). Thermal treatment (curing) for (03,08) is applied exposing samples in a L14/12/P330 muffle furnace, operated by CIEMAT solar furnace technical staff at PSA. Without coating thickness gauge, accurate dry film thickness (DFT) remains unquantified for self-applied coatings, even with a 3D confocal microscope. A typical DFT of 35 ± 15 µm is assumed, except for (09), which appeared thicker.

Uncoated H230 (01,02) is expected to oxidize and turn dark [2,11]. Pyromark 2500 (03) is a state-of the art flat black coating for CRS applications, it is expected to degrade [2,3]. Lab-IR HT (04) is a thermographic paint, its emittance is expected to change beyond 300°C. Macota 3G-HT (05) is sold in do-it-yourself (DIY) stores for chimney pipes or motorcycle exhausts, withstanding peaks up to 800°C. Cerakote Glacier BlackC-7600 Q (06) is an air cured sprayable ceramic coating designed for similar applications. Senotherm UHT600 (07), previously used in a steady-state calorimetric apparatus for hemispherical emittance measurements [16], holds up to a minimum temperature of 600 °C and is expected to degrade beyond this temperature level. Aremco high emissivity coatings (08,09) are designed for industrial furnaces [15]. Black 444 (10) is developed by Slovenia National Institute of

Chemistry (NIC) expected to degrade for prolonged above 750 °C [5]. Coterill 750 (11) is a sprayable silicon-based black paint developed by John Cockerill [6] for solar tower receivers, achieving a high solar absorptance withstanding temperatures above 700 °C. Another set of Pyromark 2500 samples (12) is supplied by John Cockerill for cross-comparison.

Optical Characterization

Spectral Reflectance Measurements

For each sample, the spectral hemispherical reflectance (SHR, [%]) is measured at room temperature, for a wavelength ranging from 0.28 to 16 µm, at a near normal incidence angle with two spectrophotometers. The SHR is measured first with the Perkin Elmer Lambda1050 spectrophotometer from 0.28 to 2.5 µm in steps of 5 nm, the incidence angle is 8°, the integrating sphere has a diameter of 150 mm, its interior is coated with Spectralon ($BaSO_4$, white diffuse), the measurement spot has a size of 7x19 mm².

This SHR measurement is extended from 2.5 to 16 µm in steps of 4 nm with a Fourier Transform Infrared (FTIR) spectrophotometer (Perkin Elmer Frontier FT-IR), the incidence angle is 12°, the integrating sphere has a diameter of 76.2 mm and its interior is coated with Infragold. The sample aperture has a diameter of 20 mm.

Both spectrophotometers overlap spectrally between 2.0 and 2.5 µm. The mismatch between both instruments, supposedly induced by different integration sphere diameters and detector types, is minimized by measuring calibrated baseline samples. Each flat sample is measured at three positions.

The analysis of spectra is further described in the next subsections. Reference spectra are shown in Fig. 1.a for calibrated sample coupons along with ideal curves for a solar selective coating (SSC) and a perfect blackbody, while weighting spectra selected for the solar absorptance and thermal emittance calculations are shown in Fig 1.b.

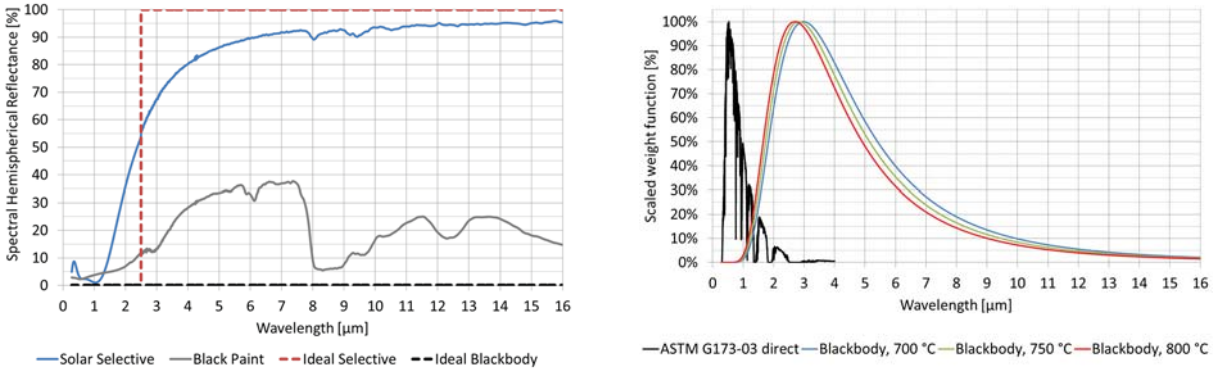

a) Reference spectra for calibration coupons

b) Weighting spectra

FIGURE 1. Reference spectra for quantitative analysis. a) Calibrated coupons (Solar selective and black paint) and ideal spectra for a solar selective coating and an idealblackbody (BB) b) Weighting spectra: Solar Spectral Irradiance (ASTM G173-03 direct+circumsolar) and blackbody radiant exitance at 700, 750 and 800°C. Weighting spectra are scaled w.r.t their maximum.

Quantitative Analysis

For quantitative analysis, the SHR measurement is first processed according to (Eq.1):

$$\rho_{sample}(\lambda) = \frac{R_{sample,meas}(\lambda)}{R_{baseline,meas}(\lambda)} \rho_{baseline,ref}(\lambda) \quad (1)$$

where λ is the wavelength expressed in nm or µm, ρ_{sample} corresponds to the sample weighted SHR, $R_{sample,meas}$ is the SHR measurement data obtained for the sample, $R_{baseline,meas}$ is the SHR measurement data obtained for the selected baseline and $\rho_{baseline,ref}$ is the reference SHR for the selected baseline, calibrated by an external laboratory (Fig.1.a.). All quantities are expressed in %.

The rules for baseline selection are primarily based on geometry and spectral properties, i.e. one should select a baseline as similar as possible to the measured sample. Otherwise, primary calibrated standards, such as Spectralon for the UV-VIS-NIR range or Infragold for the Mid Infrared (MIR) should be selected.

Solar absorptance

The solar absorptance α_{sol} [%] is calculated according to (Eq.2):

$$\alpha_{sol}(AM) = \frac{\int_{\lambda_1}^{\lambda_2} [1-\rho_{sample}(\lambda)] G_{sol}(\lambda, AM) d\lambda}{\int_{\lambda_1}^{\lambda_2} G_{sol}(\lambda) d\lambda} \quad (2)$$

where AM is the Air Mass index, G_{sol} (λ,AM) is the solar spectral irradiance shown in Fig.1.b). The reference spectrum is defined according to ASTM G173-03, AM1.5, direct+circumsolar. The wavelength ranges from λ_1 = 0.28 µm to λ_2=2.5 µm. As such, the Lambda1050 spectrophotometer delivers sufficient data for this calculation.

Thermal emittance

The thermal emittance ε_{th} [%] is calculated at a receiver temperature T (°C) according to (Eq.3) and (Eq.4):

$$\varepsilon_{th}(T) = \frac{\int_{\lambda_1}^{\lambda_3} [1-\rho_{sample}(\lambda)] M_{bb}(\lambda, T) d\lambda}{\int_{\lambda_1}^{\lambda_3} M_{bb}(\lambda, T) d\lambda} \quad (3)$$

$$M_{bb}(\lambda, T) = \frac{2\pi hc^2}{\lambda^5 [\exp(\frac{hc}{\lambda . k . T}) - 1]} \quad (4)$$

where M_{bb} is the blackbody spectral emittance in W/m^2.µm^{-1}, c, k and h are universal physical constants, which respectively correspond to the speed of light in vacuum (2.997 10^8 m.s^{-1}), Planck's constant (6.63 10^{-34} J.s) and Boltzmann's constant (1.38.10^{-23} J.K^{-1}). The wavelength ranges from λ_1 = 0.28 µm to λ_3=16 µm. As such, both spectrophotometers are required to measure the spectrum.

Opto-thermal efficiency

The coating opto-thermal efficiency $\eta_{coating}$ [%] is calculated per surface unit according to (Eq.5):

$$\eta_{coating} \simeq \frac{\alpha_{sol} \dot{q}''_{sol} - \varepsilon_{th}(T_{abs}) \sigma T_{abs}^4}{\dot{q}''_{sol}} \quad (5)$$

where $\dot{q}''_{sol}$ is the incident solar flux density (W/m^2), T_{abs} is the absorber surface temperature (°C), and σ is the Stefan- Boltzmann constant (5.67 10-8 W.m^2.K^{-4}). The numerator of this equation corresponds to the useful heat extracted from the receiver coating per unit area for a flat geometry, assuming space conditions, i.e. perfect vacuum and sky temperature at 0 K. (Eq.5) allows the definition of a trade-off factor Z between both performance indicators, with respect to the local operating point $\{T_{abs}, \dot{q}''_{sol}\}$, as described in (Eq. 6):

$$Z = \frac{\Delta \alpha_{sol}}{\Delta \varepsilon_{th}} = -\frac{\dot{q}''_{sol}}{\sigma T_{abs}^4} \quad (6)$$

For a CRS with external receiver design and a molten salt heat transfer fluid, the allowable flux density (AFD) is constrained by molten salt corrosion at high temperature [17]. The flux density varies around the receiver circumference, typically from 300 to 1000 kW/m^2. We consider a temperature range from 300 to 800 °C. In operation, high flux densities are coupled with low temperature levels, while low flux densities are coupled with high temperature levels.

The trade-off factor Z is shown in Fig. 2.a) as a function of the operating point, while the thermal emittance as a function of coating temperature is shown in Fig. 2.b) for reference coatings illustrated in Fig.1 .a). For AFD constraint outlined above, the trade-off factor ranges from 4 to 150, i.e. solar absorptance α_{sol} dominates thermal emittance ε_{th} when the solar flux density is higher than the radiative power emitted by the surface. According to Fig. 2.b), the thermal emittance for a black paint is rather not sensitive to temperature. For a selective coating, the thermal emittance range decreases as temperature increases, e.g. the thermal emittance cannot drop below 20% at 800 °C in the best ideal case.

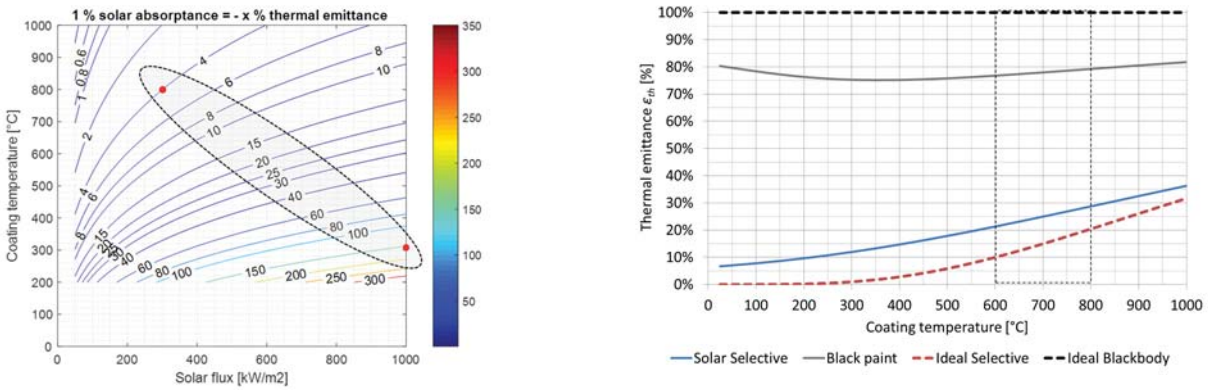

(a) Trade-off factor as a function of solar flux and temperature

(b) Thermal emittance ε_{th} as a function of temperature

FIGURE 2. (a) Trade-off factor Z as a function of solar flux and coating temperature. Isolines indicate how much the thermal emittance ε_{th} should decrease to compensate a 1% gain in solar absorptance α_{sol} to maintain a constant opto-thermal efficiency $\eta_{coating}$. (b) Thermal emittance ε_{th} as a function of coating temperature for reference coatings illustrated in Fig.1.a).

Visual Inspection

In addition to discrete spectral measurements, sample imaging is performed with a Panasonic DMC FZ45 digital camera and a Zeiss Axio CSM 700 microscope to monitor respectively millimetric and microscopic surface defects, such as corrosion spots, delamination or cracks, which are not necessarily detected by both spectrophotometers.

Isothermal Testing

Test Program

For each sample set, four samples are available for testing. One of the four samples is kept as a reference, while the other samples are respectively exposed to 700, 750 and 800 °C in a Nabertherm LT14/12/P320 muffle furnace during 1000 hours. Slow heating and cooling ramps are applied, the temperature setpoint is achieved from ambient temperature within one hour. Non-linear ramps are applied, with a maximum rate of 30 °C/min. According to Noč et al. [9], isothermal test conditions are less severe than cyclic thermal loads. The isothermal (IT) test is thus a conservative approach leading to an optimistic estimation of a receiver coating service lifetime.

Weight Measurements

All samples are weighted at room temperature before and after exposure using a Mettler Toledo ML204 analytical scale, with a resolution of 0.1 mg. This measurement allows quantifying the formation of oxide scales (mass gain) between the metal substrate and the coating. It also allows quantifying any coating degradation (mass loss), for instance delamination. Outgassing may also occur for some samples without previous thermal treatment.

RESULTS AND DISCUSSION

Visual Inspection

All samples sets are shown in Fig. 3 before and after 1000 hours isothermal exposure at 700, 750 and 800°C.

Oxidation can be visually observed on uncoated metal samples (01,02), which both appear darker after exposure, confirming previous test results [2]. According to literature [10], a duplex oxide scale consisting of Cr_2O_3 and $MnCr_2O_4$ (top) forms on the substrate surface. Optical fading is clearly visible on coatings (04,05,06), which appear gray. Coatings (03, 08-12) remain darker than oxidized substrate.

Peeling is observed for coating (07), the coating disappears after dry cleaning with pressurized air, leaving a slightly oxidized surface underneath. Before exposure, coating (09) thickness appears inhomogeneous. This

inhomogeneity is assumed to be related with the substrate selection. Coating 09 is originally designed for ceramic materials, with a higher grade of porosity. Before exposure, Coating 08 appears more homogeneous, although dark spots are locally observed after drying and curing. After exposure, both coatings (08, 09) have the same visual aspect, with similar surface inhomogeneities. A slight fading is observed on coating (10). Coating (11) appears to remains stable through testing. Coating (12) is turning darker through testing, because of curing.

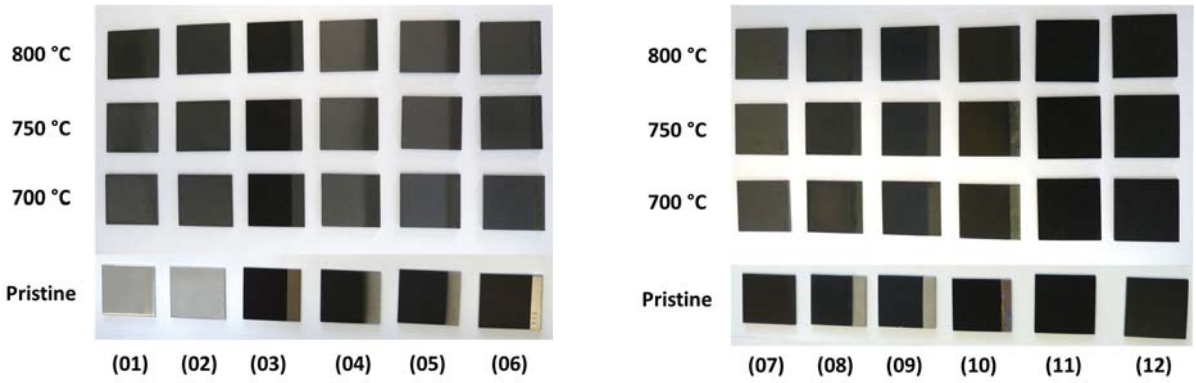

FIGURE 3. (a) Samples before exposure (b) Samples after exposure at 800 °C, 1000 hours. **Note**: The sample 00 corresponds to the bare substrate before surface treatment, it was not exposed at 800°C. It is shown for contrast.

Solar Absorptance

Solar absorptance α_{sol} before and after 1000 hours isothermal exposure is summarized for all coatings in Table 2 and Fig.4. Before exposure, only a few coatings (03,04,10,11) achieve the HSA target ($\alpha_{sol} \geq 96\%$). Slovenia NIC coating (10) is on par with Pyromark 2500 (3) (97.1%), while Coterill 750 achieves the highest α_{sol} value (97.7%). Other black coatings (05-09) as well as Pyromark (12) achieve lower values, ranging from 93.8 to 95.5%.

After isothermal exposure, observations made from the visual inspection are confirmed. Oxidized samples (01,02) achieve higher α_{sol} values, respectively up to 94.1% (1) and 93.2% (2) at 800 °C. Furthermore, the gain in solar absorptance is more pronounced at higher temperature. Oxidized samples perform better than some black coatings (04,05,07), which experience a significant loss in α_{sol}, w.r.t. pristine state Coatings (06,08, 09) achieve α_{sol} values between 90 and 95% after isothermal exposure, experiencing a milder absorptance loss w.r.t. pristine state.

Coating (10) undergoes small degradations, its α_{sol} value drops just 0.1 p.p. below the 95% threshold at 800 °C. Pyromark 2500 (03) degrades slightly, its α_{sol} value drops only by -0.7 p.p. and reaches 96.6 % at 800 °C, above the HSA target. This degradation is less pronounced as in other references [2,3,4]. Pyromark 2500 (12) cures and improves its α_{sol} value, maintaining up to 96.9%. Coterill 750 (11) leads the benchmark, its α_{sol} value remains stable above 97.5% even at 800 °C. A slight curing effect is noticed at 700 and 750 °C, as the α_{sol} value increases up to 97.9 – 98%.

TABLE 2. Solar absorptance before and after 1000 hours isothermal exposure.

ID	Coating	α_{sol}(Pristine)	α_{sol} (700 °C)	α_{sol} (750 °C)	α_{sol} (800 °C)
01	H230, polished	44.2%	85.1%	90.7%	94.1%
02	H230, sand blasted	69.0%	90.3%	91.6%	93.2%
03	Pyromark 2500 [1,2,3]	97.2%	97.0%	96.9%	96.6%
04	Lab-IR HT [11]	96.2%	87.5%	87.0%	85.6%
05	Macota 3G-HT [12]	94.8%	84.8%	83.3%	82.2%
06	Glacier Black C-7600Q [3]	93.9%	92.2%	91.7%	90.5%
07	Senotherm UHT600 [14]	93.9%	86.7%	85.0%	85.5%
08	Aremco HiE-Coat M [15]	95.5%	94.1%	95.0%	94.3%
09	Aremco HiE-Coat 840C [15]	94.3%	92.7%	94.0%	94.3%
10	Slovenia NIC, Black 444 [5]	97.1%	96.5%	95.8%	94.9%
11	Coterill 750 [6]	97.7%	98.0%	97.9%	97.6%
12	Pyromark 2500 [1,2,3]	95.5%	97.1%	96.9%	96.9%

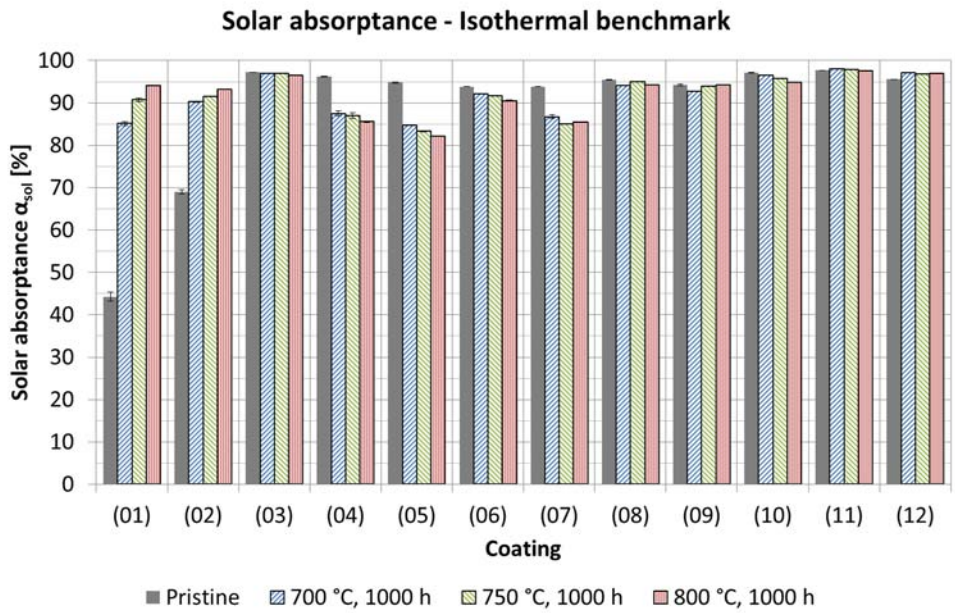

FIGURE 4. Solar absorptance before and after 1000 hours isothermal exposure.

Thermal Emittance

Thermal emittance ε_{th} (750 °C) before and after 1000 hours isothermal exposure is summarized for all coatings in Table 3 and Fig.5. Before exposure, all coated samples have a high thermal emittance ε_{th} (750 °C) of 86.5 ± 2.5%. Uncoated samples (01, 02) have a lower emittance. The polished sample achieves a ε_{th} (750 °C) value of 18.1%, while the sand blasted sample ε_{th} (750 °C) value reaches 45%.

After isothermal exposure, similar comments apply as for the solar absorptance above. Uncoated samples oxidize significantly, their ε_{th} (750 °C) value increases up to 84-85% at 800 °C. Significant deviations are recorded for coatings (04,05,07), which exhibit optical fading. Their ε_{th} (750 °C) value ranges between 73 and 84% after testing. Coatings (03,06,08-11) exhibit moderate degradation, their ε_{th} (750 °C) value range from 84 to 89% after isothermal testing. Coating (12) ε_{th} (750 °C) value increases by a few percentage points after isothermal exposure

Further spectral analysis is required to confirm ε_{th} values for coatings (04,05,08,09), as their optical properties have been investigated at operating temperature by the University of West Bohemia, Czech Republic [18,19]. Accurate knowledge of spectral emissivity at high temperature [20] is critical for the in-situ temperature monitoring of CRS using calibrated solar blind infrared imagers.

TABLE 3. Thermal emittance calculated at 750 °C before and after 1000 hours isothermal exposure.

ID	Coating	$\varepsilon_{th,750\,°C}$ (Pristine)	$\varepsilon_{th,750°C}$ (700 °C)	$\varepsilon_{th,750°C}$ (750 °C)	$\varepsilon_{th,750°C}$ (800 °C)
01	H230, polished	18.1%	67.5%	80.0%	84.9%
02	H230, sand blasted	45.0%	81.5%	82.6%	83.8%
03	Pyromark 2500 [1,2,3]	87.2%	88.7%	89.2%	88.6%
04	Lab-IR HT [11]	87.3%	78.8%	79.5%	76.1%
05	Macota 3G-HT [12]	88.3%	74.8%	74.9%	73.5%
06	Glacier Black C-7600Q [3]	88.1%	84.4%	85.1%	84.0%
07	Senotherm UHT600 [14]	81.0%	71.1%	70.5%	74.4%
08	Aremco HiE-Coat M [15]	89.6%	86.8%	87.2%	86.5%
09	Aremco HiE-Coat 840C [15]	86.9%	85.3%	85.5%	85.5%
10	Slovenia NIC, Black 444 [5]	85.6%	89.2%	89.3%	88.4%
11	Coterill 750 [6]	87.7%	90.2%	89.2%	89.4%
12	Pyromark 2500 [1,2,3]	83.1%	86.7%	88.2%	88.1%

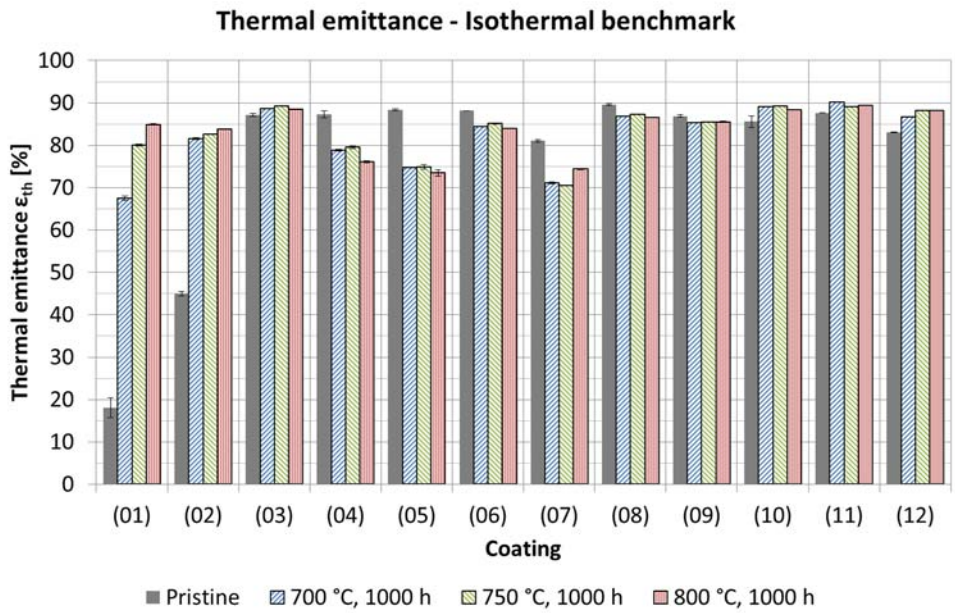

FIGURE 5. Thermal emittance before and after 1000 hours isothermal exposure.

Comparison of Sample Mass Variations

Sample mass variations are summarized in Table 4 and shown in Fig. 6 after 1000 hours isothermal exposure.

Significant mass variations can be detected on most of the samples, except for coatings (06,08). Product loss is observed on coatings (05,07,09,11). Coating (07) peeled, while coating (05,09) may have outgassed. Coating (11) has cured slightly during isothermal exposure, the mass variation is lower at higher temperature. This is more pronounced for coating (12).

Uncoated samples (01,02) gained weight due to oxidation. Coatings (03,04,10) also gained weight. One possible explanation for coatings (03,10) is the diffusion of oxygen atoms through the coating, inducing the formation of an oxide scale acting as a protective layer at the interface between the substrate and the coating [9]. Detailed metallurgical analysis would have to be carried out to confirm this hypothesis on coatings (03,10).

TABLE 4. Sample mass variation Δm [mg] after isothermal exposure.

ID	Coating	Δm (700 °C)	Δm (750 °C)	Δm (800 °C)
01	H230, polished	7.40	9.27	7.77
02	H230, sand blasted	11.60	12.43	18.60
03	Pyromark 2500 [1,2,3]	8.10	10.80	15.90
04	Lab-IR HT [11]	2.00	3.10	7.23
05	Macota 3G-HT [12]	-12.07	-13.57	-13.73
06	Glacier Black C-7600Q [3]	-5.70	-2.53	-1.53
07	Senotherm UHT600 [14]	-159.60	-154.63	-153.00
08	Aremco HiE-Coat M [15]	2.07	0.20	-1.53
09	Aremco HiE-Coat 840C [15]	-8.60	-6.63	0.20
10	Slovenia NIC, Black 444 [5]	3.70	7.57	15.57
11	Coterill 750 [6]	-53.83	-46.00	-33.40
12	Pyromark 2500 [1,2,3]	-10.67	-6.57	2.47

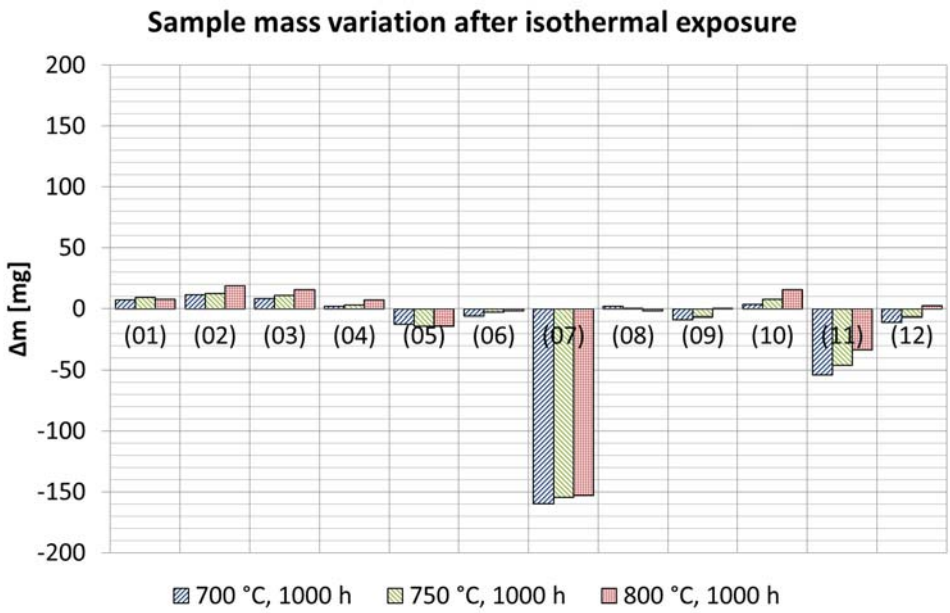

FIGURE 6. Sample mass variation after 1000 hours isothermal exposure

CONCLUSION

In this paper, a screening of high temperature (HT) sprayable black coatings applied on Haynes 230 substrate has been presented. Forty-eight samples have been characterized optically before and after 1000 hours isothermal exposure, covering a temperature range from 700 to 800 °C. Black coated samples have been compared with respect to uncoated Haynes 230 samples, which have been previously polished or sand blasted.

Before exposure, only a few coatings (03,04,10,11) achieve the HSA target ($\alpha_{sol} \geq 96\%$). Other coatings (05-09) achieved values ranging from 93.8 to 95.5%, which are suboptimal for CRS applications. All black coatings had a high thermal emittance ε_{th} (750°C) (86.5 ± 2.5%) and were not solar selective.

After isothermal exposure, uncoated samples have oxidized and achieve a solar absorptance α_{sol} of 93-94% at 800 °C. Their solar absorptance increases with temperature. Several black coated samples (04-09) showed optical fading and achieved lower values in comparison to uncoated oxidized substrates. Degradation was expected for coatings (04,07), while manufacturer claims for coatings (05,06) were ambiguous. The degradation of coatings (08-09) may have been induced by inappropriate coating application.

Among HSA candidates, coating (10) showed a minor loss of optical performance after 1000 hours at a temperature above 700 °C, maintaining a solar absorptance α_{sol} of 96.5%. Pyromark 2500 (03) degraded slightly, however the degradation rate was less pronounced as published in other references. With a different application and curing procedure (12), a curing could be observed and a solar absorptance α_{sol} of 96.9% could be achieved after 1000 hours. Coterill 750 (11) leads the benchmark, with a stable solar absorptance α_{sol} above 97.5% up to 800 °C. In order to build a service lifetime prediction, further testing would have to be conducted to take into account cyclic thermal loads and concentrated solar radiation.

Further experiments are scheduled within the SFERA3 EU research project in order to measure the spectral emissivity of oxidized Haynes 230 and aged Pyromark 2500, both at ambient and operating temperature, between 200 and 800 °C. This knowledge is critical for the development of a multichromatic thermographic measurement system, allowing in-situ receiver surface temperature measurements and receiver degradation monitoring.

ACKNOWLEDGMENTS

Financial support from the European Union is gratefully acknowledged (EU-SFERA3 project, Horizon 2020, Contract n° 823802). The main author thanks all participating companies for supplying their coating, the OPAC laboratory technical staff: Lucia Martinez, Carmen Amador and Tomas Reche for their technical assistance in optical measurements and isothermal muffle furnace testing, David Muruve and Jose Galindo for their support during sample preparation.

REFERENCES

1. C.K. Ho et al., "Characterization of High-Temperature Solar Receivers", *Journal Solar Energy Engineering*, **136**, 041502-1:4 (2014).
2. J. Coventry, P. Burge, "Optical properties of Pyromark 2500 coatings of variable thickness on a range of materials for concentrating solar thermal applications", *AIP Conference Proceedings*, **1850**, 030012 (2017).
3. A. Ambrosini et al., " Influence of application parameters on stability of Pyromark® 2500 receiver coating", *AIP Conference Proceedings,* **2126**, 030002 (2019).
4. K. Tsuda et al., "Development of high absorption, high durability coatings for solar receivers in CSP plants", *AIP Conference Proceedings,* **2033**, 040039 (2018).
5. I. Jerman et al., "Merging of oxide species with black spinel structure by CSP operating temperature", *AIP Conference Proceedings*, **2033**, 220002 (2018).
6. R. Harzallah et al., "Development of high performances solar absorber coatings", *AIP Conference Proceedings*, **2126**, 030026 (2019).
7. C. K. Jo, J. Pacheco, "Levelized Cost of Coating (LCOC) for selective absorber materials", *Solar Energy*, **108**, 315-321 (2014).
8. A. Boubault et al., "Durability of solar absorber coatings and their cost-effectiveness", *Solar Energy Materials & Solar Cells*, **166**, 176-184, (2017).
9. Luka Noč et al., "High-solar-absorptance CSP coating characterization and reliability testing with isothermal and cyclic loads for service-life prediction", Energy & Environ. Sci., **12**, 1679-1694, (2019).
10. Li Jian et al., "Oxidation kinetics of Haynes 230 alloy in air at temperatures between 650 and 850 °C", Journal of Power Sources, **159**, 641-645, (2006).
11. LabIR-HT: https://paints.labir.eu/paint/thermographic-paint-for-high-temperature-applications
12. Macota 3G-HT: https://www.macotasrl.it/en-gb/heat-resistant-paints
13. Cerakote C-7600Q: https://www.cerakotehightemp.com/finishes/C-7600Q/cerakote-glacier-black/
14. Senotherm UHT: https://www.senotherm.com/produkte/senothermr-uht/
15. Aremco High Emissivity Coatings: https://www.aremco.com/high-emissivity-coatings/
16. T. Effertz, et al., "Steady-State calorimetric measurement of total hemispherical emittance of cylindrical absorber samples at operating temperature", AIP Conference Proceedings, **1850**, 020003 (2017).
17. L.L. Vant-Hull, "The Role of "Allowable Flux Density" in the Design and Operation of Molten Salt Solar Central Receivers", Journal of Solar Energy Engineering, **124**, 165-169, (2002).
18. P. Honnerova, et al., "New experimental device for high-temperature normal spectral emissivity measurements of coatings", *Meas. Sci. Technol.*, **25**, 095501 (2014).
19. P. Honnerova, et al., "Uncertainty determination in high-temperature spectral emissivity measurement method of coatings", *Applied Thermal Engineering*, **124**, 261-270 (2017).
20. E. Le Baron, et al., "Round Robin Test for the measurement of spectral emittance measurement apparatuses", *Solar Energy and Material Cells*, **191**, 476-485, (2019).